Frontiers in Life Science
Publication details, including instructions for authors and subscription information:
http://www.tandfonline.com/loi/tfls20

Histone modifications control DNA methylation profiles during ageing and tumour expansion

Jens Przybilla[a], Peter Buske[b], Hans Binder[a] & Joerg Galle[a]

[a] Interdisciplinary Center for Bioinformatics, University Leipzig, Leipzig, Germany

[b] Institute for Medical Informatics, Statistics and Epidemiology, University Leipzig, Leipzig, Germany

Published online: 12 Dec 2013.

To cite this article: Jens Przybilla, Peter Buske, Hans Binder & Joerg Galle (2013) Histone modifications control DNA methylation profiles during ageing and tumour expansion, Frontiers in Life Science, 7:1-2, 31-43, DOI: 10.1080/21553769.2013.854279

To link to this article: http://dx.doi.org/10.1080/21553769.2013.854279

Frontiers in Life Science, 2013
Vol. 7, Nos. 1–2, 31–43, http://dx.doi.org/10.1080/21553769.2013.854279

Taylor & Francis
Taylor & Francis Group

Histone modifications control DNA methylation profiles during ageing and tumour expansion

Jens Przybilla[a], Peter Buske[b], Hans Binder[a] and Joerg Galle[a]*

[a]*Interdisciplinary Center for Bioinformatics, University Leipzig, Leipzig, Germany;* [b]*Institute for Medical Informatics, Statistics and Epidemiology, University Leipzig, Leipzig, Germany*

(*Received 9 July 2013; final version received 8 October 2013*)

The stem cell epigenome reflects a delicate balance of chromatin (de-)modification processes. During cancer development this balance becomes disturbed, resulting in characteristic changes. Among them are changes of the DNA methylation profile. It has been demonstrated that these changes share common features with changes observed during stem cell ageing. Recently, we proposed that chromatin remodelling during stem cell ageing originates in the limited cellular capability to inherit histone modification states, and thus is linked to cell proliferation. This suggests that increased proliferation activity and associated loss of histone modification may represent a generic cause of the changes observed in cancer DNA methylation profiles. Moreover, additional changes of these profiles due to mutations of chromatin modifiers are expected to act on this background. We study the implications of these assumptions, introducing a computational model which describes transcriptional regulation by cis-regulatory networks, trimethylation of histone 3 at lysine 4 and 9 and DNA methylation. By simulation of the model we analyse how mutations that change the proliferation activity and histone de-modification rates impact DNA methylation profiles. We demonstrate that our hypotheses are consistent with experimental findings, and thus may provide a mechanistic explanation of DNA methylation changes during ageing and tumour expansion.

Keywords: DNA methylation; histone modification; H3K4me3; H3K9me3; stem cell ageing; tumour expansion

Introduction

During development and differentiation, chromatin undergoes global remodelling. This process involves modification both of histones and DNA. Histone modifications can be rapid, on a timescale of seconds to hours (Hayashi-Takanaka et al. 2011), being accompanied by rapid changes in gene expression. These changes are, however, largely reversible. In contrast, changes in DNA methylation require cell proliferation (Velicescu et al. 2002) and confer long-term gene silencing that can be stable for months or years (Raynal et al. 2012).

There is increasing evidence for an intimate cross-talk between histone modifications and DNA methylation (D'Alessio & Szyf 2006). For example trimethylation at lysine 4 of histone 3 (H3K4me3) directly suppresses recruitment of DNA methyltransferases (DNMTs) (Ooi et al. 2007) and, in turn, DNA methylation impairs recruitment of the histone methyltransferases (HMTs) of H3K4me3 (Thomson et al. 2010). Conversely, trimethylation at lysine 9 of histone 3 (H3K9me3) has been suggested to recruit DNMTs (Feldman et al. 2006) and H3K9 HMTs have the potential to bind to methylated DNA (Fujita et al. 2003). We here focus on this kind of interplay and look at its role during ageing and tumour expansion.

We hypothesize that the observed changes of the DNA methylation profile originate in changes of the modification status of associated histones. In order to support this idea, we studied these processes in computer simulations (*in silico*), where all properties of the system are in our hands. For this purpose we introduced an artificial genome-based computational model of epigenetic regulation during ageing and tumour expansion based on a multi-scale model of transcriptional regulation (Binder et al. 2013).

Ageing has been demonstrated to be accompanied by genome-wide changes in epigenetic states. Recently, we proposed a model of epigenetic ageing that is capable of explaining such changes, assuming a limited inheritance of the histone modifications H3K4me3 and H3K9me3 that control DNA methylation by the mechanism mentioned above. In particular, the model is capable of explaining age-related local hyper- and global hypo-methylation of the DNA (Przybilla et al. 2012). Such epigenetic changes have been suggested by many experimentalists to increase susceptibility to tumour development. They provide a possible explanation for age, being the greatest risk factor for cancer. In fact, it has been demonstrated that these changes share common features with changes observed in cancers. For example, Teschendorff et al. (2010) observed that the

*Corresponding author. Email: galle@izbi.uni-leipzig.de

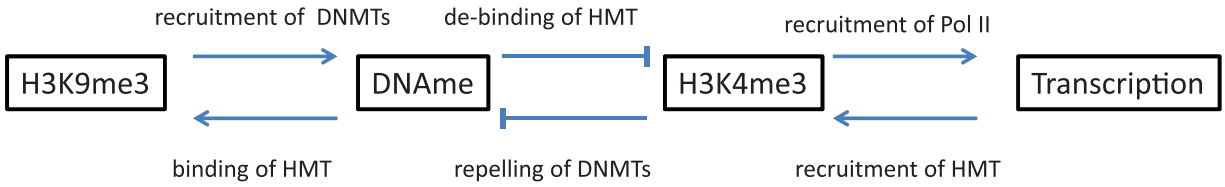

Figure 1. (Colour online) Sketch of the regulatory principals of the model. A negative feedback loop between H3K4me3 modification and DNA methylation and a positive one between H3K9me3 modification and DNA methylation control the epigenetic states of the system. Another positive feedback loop between H3K4me3 and transcriptional activity links the TF network to the epigenetic regulation layers.

genes that become methylated during ageing are genes frequently methylated in cancers. Here, the question arises of whether hyper-methylation during ageing and tumour expansion actually originates from similar or even the same regulatory processes. The fact that tumour expansion is accompanied by activated cell proliferation, led us assume that active proliferation itself represents a generic cause of such alterations of DNA methylation.

We hypothesize that the changes observed during tumour expansion are a consequence of limited inheritance of histone modifications, in the same way as in ageing tissue. In other words, we expect fast expansion of dominant clones to be paralleled by accelerated ageing of these clones that manifests in their DNA methylation profiles. Accordingly, we expect the timescales of histone modification and cell proliferation to play an essential role in controlling methylation profiles during both ageing and tumour expansion. Combining our model of epigenetic regulation with an individual cell-based model of cell populations allows us to simulate these processes on the molecular, cellular and population level.

Mutations of chromatin modifiers may either support or repress age-related epigenetic remodelling during tumour expansion. In two exemplary simulation studies we here analyse deregulation of histone demethylases (HDMs) for H3K9 and H3K4; members of which have been found deregulated in cancers. For example, loss of KDM4C, an H3K9 HDM, is known to induce methylator phenotypes in glioblastoma (Turcan et al. 2012) and acute myeloid leukaemia (Akalin et al. 2012). Overexpression of KDM5A, an H3K4 HDM, is associated with tumour cell proliferation and drug resistance in breast cancers (Hou et al. 2012). Applying our computational model we provide hypotheses on changes of the methylation profiles following these mutations.

Results

Model design

In order to study processes of deregulated DNA methylation during ageing and tumour expansion *in silico*, we extended a multi-scale model of transcriptional regulation by histone modifications recently developed by us (Przybilla et al. 2012; Rohlf et al. 2012). The model describes transcriptional regulation within a cell carrying an artificial genome (AG) (Reil 1999). The genes of the AG define a transcription factor (TF) network. Gene regulation by this network is considered by explicitly modelling TF binding and interaction with polymerase II bound to the base promoter of the genes (Binder et al. 2010). In addition gene regulation is controlled by histone modification and DNA methylation. Histone modification is described as a balance between permanent modification and de-modification reactions of the histones of cooperative acting nucleosomes (Binder et al. 2013). We consider two different histone methylations, namely H3K4me3 and H3K9me3. The reactions catalyzing these modifications have both been shown to be controlled by a reader–writer positive feedback loop which enables bistable modification states. This bistability depends on the number of adjacent, cooperatively acting nucleosomes given as the length of the cooperative unit (CU, see Appendix), and on the methylation state of the associated DNA. The latter can change in the model only due to limited maintenance and potential *de novo* methylation during cell replication (Sontag et al. 2006; Przybilla et al. 2012). DNA *de novo* methylases are assumed to be recruited by H3K9me3 (Feldman et al. 2006) and repelled by H3K4me3 (Ooi et al. 2007). Changes of the H3K4me3 state are assumed to impact transcription of associated genes by changing their promoter activity proportional to the binding probability of the complex catalyzing this modification. DNA methylation impacts transcription only indirectly by changing this complex binding probability. We assume the catalytic complexes of H3K4me3 to bind to unmethylated CpGs (Thomson et al. 2010) and the catalytic complexes of H3K9me3 to bind to methylated CpGs (Fujita et al. 2003). As the latter recruit DNA methylases, this assumption defines a positive feedback loop of DNA methylation. A sketch of the regulatory principals of the model is shown in Figure 1. Details can be found in the Appendix.

Genes that become hyper-methylated during ageing and tumour development are frequently genes with low expression in normal tissue (Sproul et al. 2011; Takasugi 2011). So, why are genes expressed in normal tissue effectively protected from hyper-methylation? According to our former hypothesis (Przybilla et al. 2012) hyper-methylation is a consequence of H3K4me3 loss. Thus, the question is what stabilizes H3K4me3 at expressed genes. A possible answer is that the recruitment of H3K4 methylases is enforced at transcribed promoters. This would lead to a positive feedback stabilizing H3K4me3 at these chromatin regions. Indeed, experimental findings suggest such a mechanism:

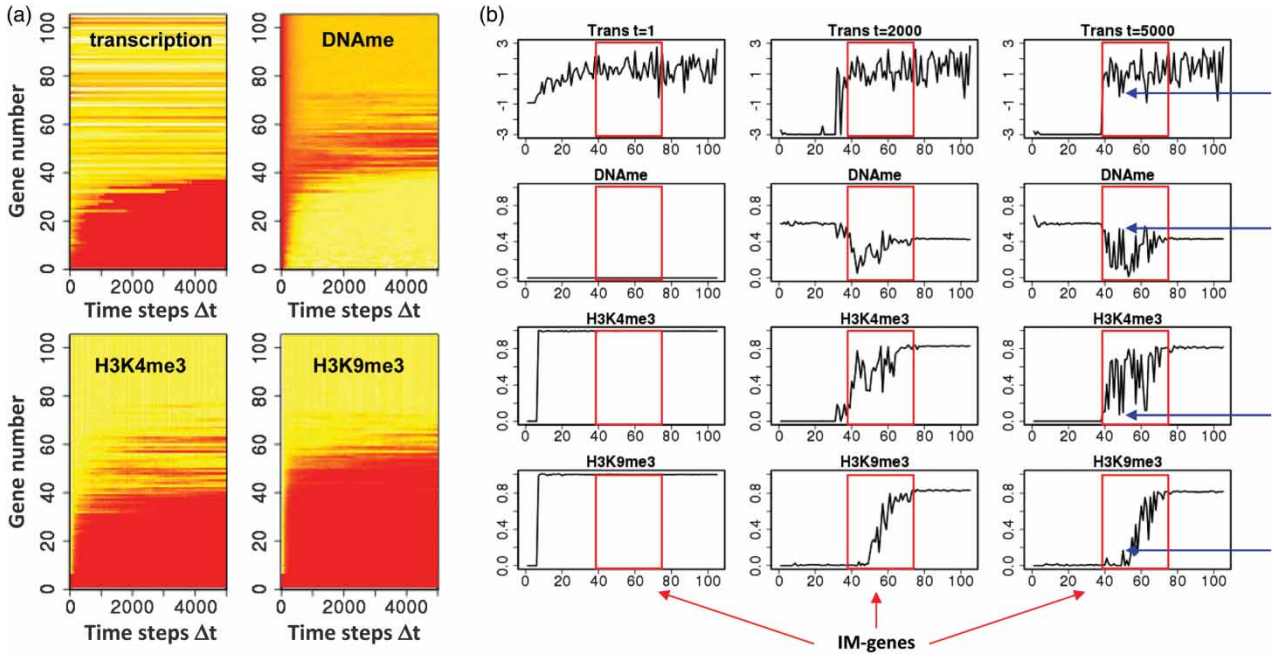

Figure 2. Simulated age-related changes in the epigenome. Shown are results for low rates of histone (de-) modification as a function of simulation time. (a) Regulatory states for each gene are averaged separately over all cells in the population (red–yellow–white: low–high, 100 time steps Δt refer to one generation). Genes are sorted in each plot according to their length, increasing from bottom to top. Transcription is given as log-values, histone modification and DNA methylation as the fraction of modified nucleosomes and methylated CpG sites associated with the gene, respectively. Over time a defined regulatory profile develops. (b) Profiles of the regulatory states at selected time points. For short genes (up to no. 39) and long genes (larger than no. 75) epigenetic states are largely independent of transcription. For IM genes (red boxes) the TF network modulates the regulatory states. The blue arrows indicate e.g. three genes of nearly equal length that differ in expression. The low expressed ones show high DNA methylation due to vanishing H3K4me3.

The C-terminal domain (CTD) of the RNA polymerase II subunit Rpb1 undergoes dynamic phosphorylization. During early elongation, CTD serine 5 phosphorylization helps to recruit the H3K4 HMT complex containing Set1 (Buratowski & Kim 2010). In line with these arguments, we here assume that the recruitment of H3K4 HMTs depends on the transcriptional activity of the associated gene. We assume an energy term governing the HMT recruitment proportional to the logarithm of the transcription. Details are again found in the Appendix.

We are aware of a much more complex interplay between the agents of the system, e.g. due to HMT-HDM interactions (Chaturvedi et al. 2012). Moreover, histone modifications other than H3K4me3 and H3K9me3 affect DNA methylation (see Discussion). For sake of simplicity, we neglect these regulatory layers in our model.

Model simulation

In our model simulations we followed the development of the regulatory states in cell populations. Each cell of a population is characterized by its specific time-dependent transcriptional, histone modification and DNA methylation profile. We summarized these profiles in the matrix $\{\mathbf{T}, \mathbf{A}, \mathbf{B}, \mathbf{M}\}$, where **T**, **A**, **B**, and **M** are vectors of length N, describing the transcription, H3K4me3, H3K9me3 and DNA methylation level of all N genes of the genome. We assumed that in the initial state of the system all nucleosomes are H3K4me3 modified ($\mathbf{A} = \{1\}$) and all CpGs are unmethylated ($\mathbf{M} = \{0\}$) (see Discussion). We varied the histone modification level of H3K9me3 assuming that all histones are either completely modified ($\mathbf{B} = \{1\}$) or completely unmodified ($\mathbf{B} = \{0\}$). Thus, we performed simulations with two different initial conditions. The transcription level of the genes depends on the H3K4me3 level. Accordingly, all simulations were started with the same initial transcription status, **T1**.

Age related changes of the epigenome

In a first series of simulations, we analysed the behaviour of cell populations that age according to the assumptions made in our model and identified characteristic features of this ageing process. Figure 2A shows typical simulation results for a system with the initial conditions (**T1**, {1}, {1}, {0}). After a short equilibration time of less than 500 time steps (Δt) the regulatory state of many genes becomes largely stable. Only a few genes, associated with CUs of intermediate length, continue to undergo changes on a longer timescale ($> 1000\Delta t$). In the following we call these genes 'age-related genes'. Moreover, genes associated with a short, intermediate, or long CU will be called 'short', 'intermediate' and 'long' genes, respectively.

The observed behaviour can be explained as follows (Przybilla et al. 2012): in the case of short genes histone modification is not stable and the initial high H3K4me3 and H3K9me3 modification level is immediately lost. Longer genes keep their modification. However, during replication the histones of the mother cell are randomly distributed onto the daughter cells and complemented with unmodified histones, resulting in strong dilution of modified histones (Binder et al. 2013). Thereby, dilution of H3K4me3 modified histones opens time windows for DNA methylation, which is otherwise prevented by this modification. This DNA methylation weakens H3K4me3 modification and stabilizes the unmodified H3K4me3 state. Thus, over longer times H3K4me3 is lost. This behaviour defines a first group of age-related genes: AG1. Above a certain gene length this process stops and H3K4me3 remains largely stable. Whether the DNA associated with the respective genes remains unmethylated is determined by the H3K9me3 modification state. Like H3K4me3, H3K9me3 stabilizes for long genes. Thus, both marks are found on long genes and the associated DNA becomes modestly methylated. For the chosen parameter set, we observed a group of genes (nos. 39 to 75) where H3K4me3 is stable but H3K9me3 is not and the DNA remains unmethylated. In the following, we call these genes intermediate (IM) genes.

The longest IM genes lose H3K9me3 only slowly. Thus, in an initial phase the remaining H3K9me3 recruits DNMTs and the DNA becomes methylated, but in the long term the DNA becomes again demethylated. This behaviour of transient DNA methylation defines a second group of age-associated genes: AG2. Together the behaviour of AG1 and AG2 genes can explain the age-related phenomenon of parallel DNA hyper- and hypo-methylation.

In general, the described ageing process is a result of the limited inheritance of the histone marks and originates in their dilution during replication. Ageing will be retarded for faster histone modification dynamics, shortening the time windows for DNA methylation after replication. Conversely, it will be accelerated for slower histone modification dynamics, lengthening these windows. We demonstrated this behaviour in simulations where we assumed that both histone modification and de-modification processes occur with a 10-fold higher rate compared to the simulations shown in Figure 2. A simulation example can be found in the Appendix (Figure A1). Under these conditions the stationary solutions of the system remain unchanged (Binder et al. 2013). Nevertheless, AG1 and AG2 genes identified under low (de-) modification conditions now conserve H3K4me3 and H3K9me3, respectively. Thus, the numbers of AG1 and AG2 genes decrease, i.e. the regulatory states no longer show age-related changes.

Notably, some of the described phenomena depend on the initial conditions chosen. So, for the chosen parameter set and for the analyzed gene lengths, stable H3K9me3 modification does not establish for (**T1**, {1}, {0} {0}. A simulation example of the latter scenario can be found in the Appendix (Figure A2). All phenomena described so far can be rationalized in terms of the cooperative nature of the histone modification reactions. Interestingly, not all genes, in particular not all IM genes, behave as expected reflecting additional regulation mechanisms. Actually, some IM genes become DNA methylated. This is a consequence of the feedback of transcription on histone modification. According to our assumption, gene expression stabilizes H3K4me3 modification. Thus, repressed genes de-modify more easily than activated genes. As a consequence, the DNA methylation profile is modulated by the TF network. Figure 3 shows some details on DNA methylation of IM genes. It demonstrates that low expressing genes are enriched in the set of genes the DNA of which becomes highly methylated. Thus, our model nicely describes the results of Takasugi (2011).

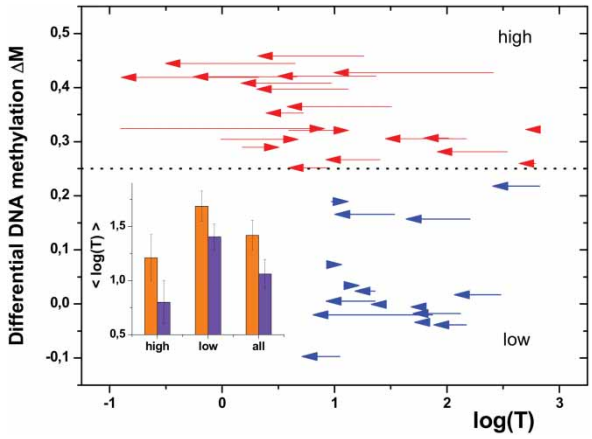

Figure 3. Transcription modulates DNA methylation. Shown is the differential methylation ΔM of the IM genes specified in Figure 2. The vertical axis specifies $\Delta M = M(5000\Delta t) - M(100\Delta t)$. The horizontal arrows specify the change in transcription connecting $\log(T)$ at $t = 100\Delta t$ and $5000\ \Delta t$ (arrow head). Genes becoming strongly hypermethylated (red) are often initially ($t = 100\Delta t$) low expressing genes, most of them becoming further repressed. The insert compares the average initial transcription of all genes with that of genes with high ($\Delta M > 0.25$) and low ($\Delta M < 0.25$) differential methylation at $t = 100\Delta t$ (yellow) and $t = 5000\Delta t$ (violet). Errors are SEMs.

Mutation related changes of the epigenome

We performed a second series of simulations, in order to demonstrate how specific mutations affect the behaviour of ageing cell populations. We start with mutations that accelerate proliferation and thus generate competitive clones. A clone mutated in this way will overgrow the system and induce monoclonality. Figure 4 shows simulation results illustrating the consequences of such a mutation on the ageing process. We assumed that the proliferation rate in the mutated clone is increased by 20%. As expected, the mutated clone overtakes the system after its occurrence. Thereby, it enforces fast silencing of age-related genes. This accelerated ageing is based on enforced H3K4me3 destabilization in the course of faster proliferation. The process

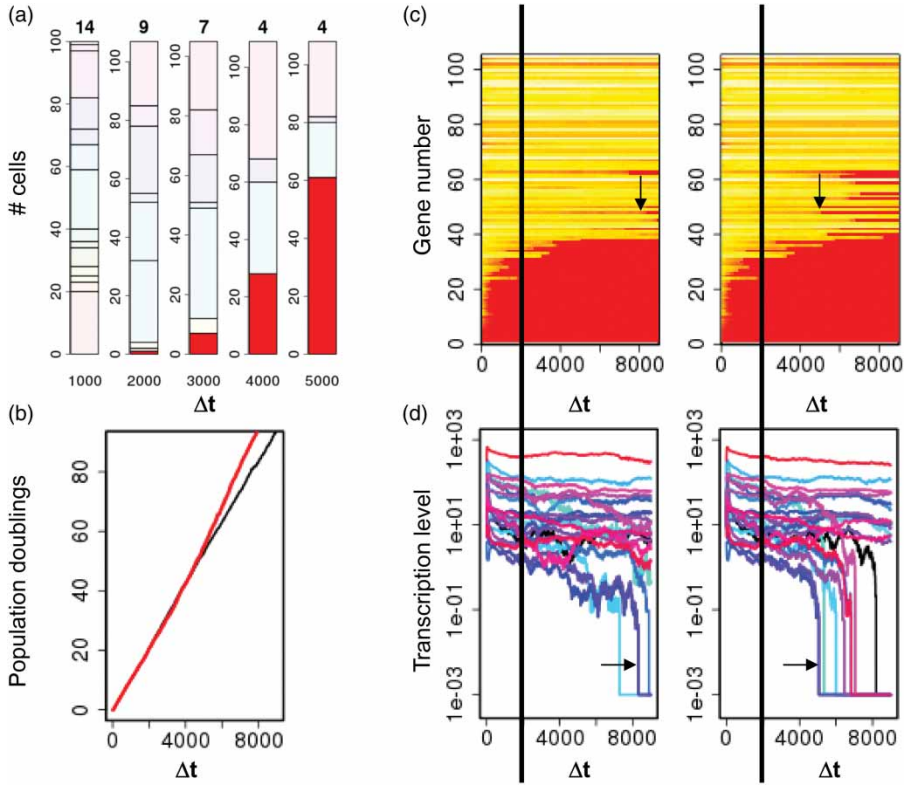

Figure 4. Simulated accelerated ageing in hyperplastic tissue. (a) Clonal development. Numbers at the left indicate the cell numbers, number on top the number of clones present, and the number at the bottom indicate the time point in Δt. The red colour indicates the hyper-proliferative clone, that was initialized at $t = 2000\Delta t$ (black lines in c and d). This clone enforces a higher turnover of the system. (b) Number of population doublings in a normal ageing system (black line) and the system, with the mutated clone (red line). (c) Averaged transcription level (colours and averages as in Figure 2a) of all genes without (left) and with (right) the hyper-proliferative clone. Gene silencing is clearly accelerated in presence of the hyper-proliferative clone (arrows highlight a representative gene). (d) Explicit view on the transcription level of the intermediate genes. Each colour labels a different gene. Arrows highlight the same gene as in (c).

not only runs on shorter timescales but applies also to additional genes. This suggests that the experimental finding that the genes that become methylated during ageing are genes frequently methylated in cancers (Teschendorff et al. 2010) may be due to a similar molecular process running in ageing and tumour cells.

During tumour expansion H3K4me3 can be further destabilized by mutations of histone modifiers. Although such mutations do not directly lead to a competitive phenotype they are observed in several tumour subtypes. An example of such a subtype is that of a glioblastoma carrying IDH1/2 mutations (Lu et al. 2012; Turcan et al. 2012). The related phenotype is called a methylator phenotype, as many genes become hyper-methylated. It has been demonstrated that these changes originate from changes in the activity of the H3K9 HDM KDM4C following IDH1/2 mutation (Lu et al. 2012).

We simulated such a mutation, assuming that at a certain time point the H3K9 HDM activity vanishes. The clone of a single mutated cell would frequently die out because the mutation is not linked to a competitive phenotype. So, we simulated the changes of the regulatory states following the mutation, assuming that the H3K9me3 HDM activity approaches zero at a certain time point in all cells of the population under consideration, i.e. we simulated a large mutated clone.

We complemented our simulation series on the H3K9 HDM activity with analogue simulations where we assumed the H3K4 HDM activity would vanish. Such a scenario may be observed following mutations of the H3K4 HDMs (Grafodatskaya et al. 2013). Alternatively, it could be induced by changes in the oxygen tension which is known to regulate KDM5A (Zhou et al. 2010). We asked whether a knock-down of H3K4 HDMs, stabilizing H3K4me3, is able to retard the ageing processes or can even partly reverse it.

As expected, the assumed knock-down of the H3K9 (H3K4) HDM activity increased H3K9me3 (H3K4me3) levels in several regions of the genome. As a consequence the DNA profiles changed as well. Simulation results are shown in the Appendix (Figure A3). They demonstrate that regulatory states different from that of a normal aged cell are observed following such knock-down. A detailed analysis of the simulation results is provided in the next section.

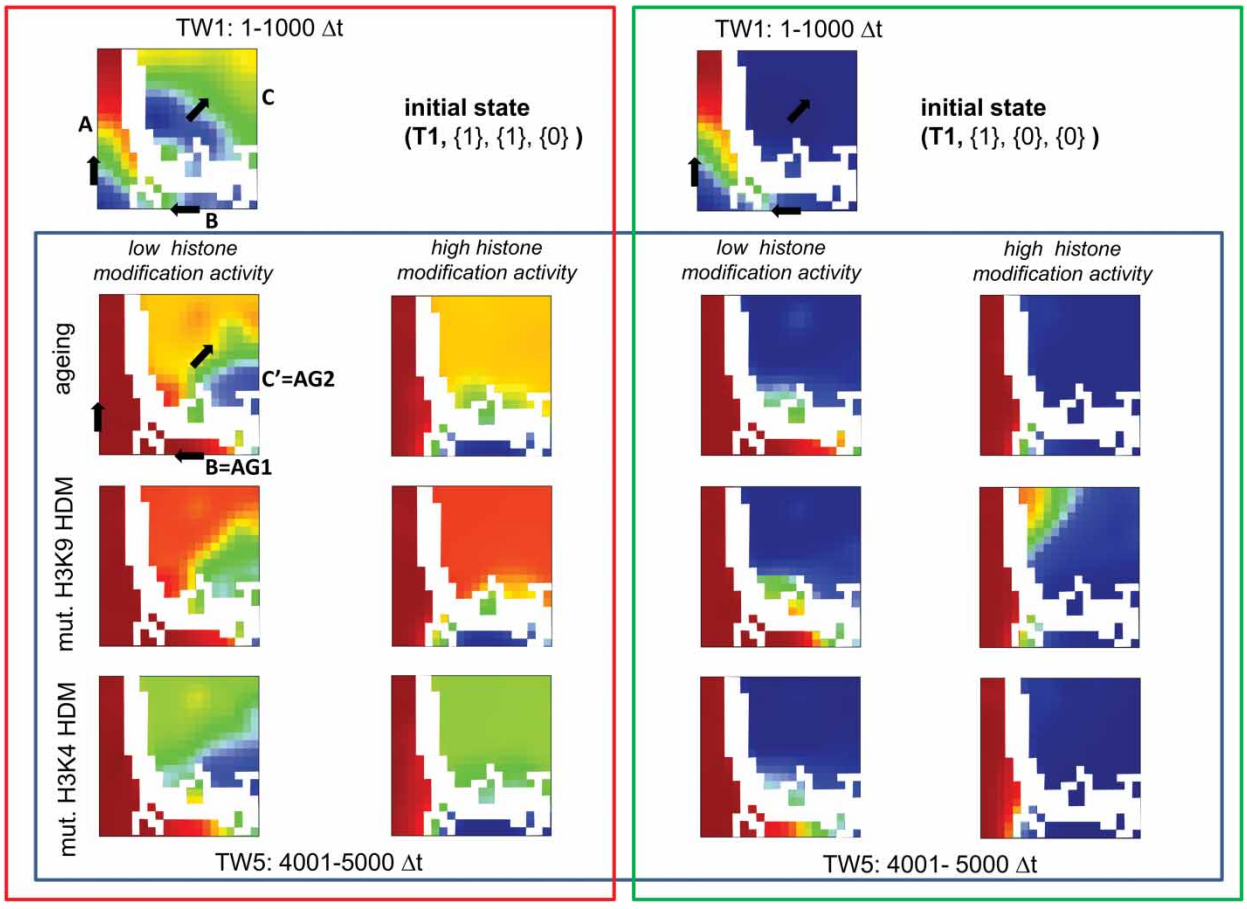

Figure 5. Integrated SOM analysis of DNA methylation. Shown are selected SOM portraits for the initial conditions (**T1**, {1}, {1}, {0}) (red box) and (**T1**, {1}, {0}, {0}) (green box). The two single portraits are portraits of the TW1 for normal ageing under low histone (de-) modification activity. The two groups of six portraits (blue box) are portraits of all scenarios for TW5. All portraits show white areas referring to empty meta-elements not populated with a single element. These white areas separate clusters A, B and C of meta-elements. At TW5 genes associated with these clusters are: (A) methylated under all conditions, (B) methylated for low histone (de-) modification activity only, and (C) methylated for initially high H3K9me3 level only. Within the clusters the meta-elements arrange according to the average time point of the associated elements. Black arrows indicate progressive time. Note that the portraits of TW1 reveal fast methylation of genes associated with cluster A. AG1 and AG2 genes are associated with cluster B and the blue sub-region C′ of cluster C, respectively.

Integrated analysis of methylation profiles

In order to interlink the changes in DNA methylation observed during ageing and after mutation we performed an integrated analysis using a self-organising map (SOM). The SOM was trained with the methylation values of all genes at all time points and for all scenarios listed in Table A1. Each of the 12 scenarios was subdivided into five time windows (TW) of 1000 Δt (1–1000 Δt,…, 4001–5000 Δt). Thus, we defined 12 × 5 data matrixes, each containing the methylation values of all genes ($i = 1, \ldots, N$) at 1000 sequential time points ($j = 1, \ldots, 1000$). The methylation levels of an matrix element (i, j) across all the 60 matrixes define its SOM profile. Applying the SOM algorithm the matrix elements become grouped to meta-elements serving as the prototypic SOM profile of the associated elements. These meta-elements arrange on a 2D grid (20 × 20) such that most similar meta-elements become neighbours. Each data matrix is then visualized by its SOM portrait, colour-coding the methylation level of each meta-element in the particular matrix (blue–green–red assigns low to high methylation levels). The gallery of all portraits obtained is given in the Appendix (Figure A4).

Figure 5 shows selected portraits of this gallery. The SOM algorithm separated three main clusters of meta-elements referred to as A, B, and C, which differ in their DNA methylation owing to different histone (de-)modification rates and different initial conditions. Regions between these clusters are separated by white depopulated areas. In each of the three clusters the meta-elements arrange according to the average time point (j) of the associated elements. Thus, the method allows short-term methylation changes to be followed in each portrait. Arrows in the portraits point in direction of progressive time (for details see Appendix, Figure A5). Invariant colouring along these arrows indicates equilibrated steady-state methylation, whereas changing colour indicates ongoing

alterations. The portraits of TW1 clearly reveal strong methylation changes, while portraits of TW5 indicate steady state methylation.

Ageing. The results of the SOM analysis, first of all, recapitulate those observed for the ageing process in the individual simulations. The meta-element clusters separate different groups of genes that have been identified based on the dynamics of the regulatory states described above. Genes associated with cluster **A** became almost completely methylated within the first 1000 time steps. As seen from the portraits of TW1 these changes are largely independent of the initial conditions (and of the histone (de-) modification activity; not shown). The gene length map given in the Appendix (Figure A5) shows that cluster A mainly contains the short genes that immediately lose H3K4me3 and H3K9me3. Genes associated with cluster **B** behave similarly but on a longer timescale and only for low histone (de-) modification activity. These genes are slightly longer than those of cluster A. They mostly belong to the AG1 group. Genes associated with cluster **C** are longer genes. They rarely show DNA methylation for (**T1**, {1}, {0}, {0}) conditions, while for (**T1**, {1}, {1}, {0}) they show a more complex methylation behaviour. A subgroup of these genes, located in region **C**′, comprises the AG2 genes, showing characteristic transient methylation.

Based on these SOM results a simple summary of the changes observed in the course of H3K9 and H3K4 HDM knock-downs can be provided, as detailed next.

Mutation in the H3K9 HDM. This mutation has a strong effect on genes associated with cluster **C**. However, this effect is observed for the initial state (**T1**, {1}, {1}, {0}) only. Under these initial conditions all **C** genes become hyper-methylated compared to normal ageing, independent of the histone (de-) modification activity, i.e. genes of group AG2 also become methylated. In case of slow (de-) modification the effect thus overwrites the hypo-methylation phenomenon observed during normal ageing. For (**T1**, {1}, {0}, {0}) the mutation has an effect for fast histone (de-)modification activity only. Here, H3K9me3 stabilizes at the longest genes and the associated DNA becomes progressively methylated in the long term.

Mutation in the H3K4 HDM. This mutation also has a strong effect on genes of cluster **C**. Here, all **C** genes become hypo-methylated compared to normal ageing, independent of the histone (de-) modification activity. As **C** genes are not methylated for (**T1**, {1}, {0}, {0}), the effect is again seen for (**T1**, {1}, {1}, {0}) only. For slow histone (de-) modification activity the mutation suppresses neither hyper-methylation of AG1 genes (cluster **B**) nor hypo-methylation of AG2 genes (region **C**′). Thus, the mutation does not 'rejuvenate' the cells. For fast modification activity it resets **C** genes to an early methylation state ($t \sim 500\Delta t$), and thus supports the preventive effects of this modification regime. For (**T1**, {1}, {0}, {0}) effects of the mutation are rarely observed.

Discussion

Changes of DNA methylation during ageing and tumour development are documented for many tissues and tumour types. However, the origin of these changes is still a matter of debate. The multi-scale model proposed here links DNA methylation dynamics to histone modification states. This is achieved by linking the recruitment of DNMTs to the local histone modification state.

During ageing these states can change in proliferative cells due to their limited inheritance. In the case of H3K4me3 loss this will enable DNA hyper-methylation of the associated genes that are otherwise protected (Ooi et al. 2007). In the case of H3K9me3 loss this impairs recruitment of *de novo* DNMTs (Cedar & Bergman 2009) and will lead to passive hypo-methylation. According to our model the properties of the histone machinery but also the ratio between the timescale of histone (de-) modification and proliferation control whether a particular gene will be affected by these mechanisms. The model suggests ageing in hyperplastic tissue to be accelerated in general. This is in agreement with experimental findings that genes hyper-methylated in ageing tissue are hyper-methylated in related tumours as well (Teschendorff et al. 2010).

A direct comparison of DNA methylation changes in fast and slow proliferating cells of the same origin is currently missing. However, the results on HSC ageing obtained by Beerman et al. (2013) that ageing of HSCs is associated with alterations of DNA methylation that accumulate with the number of cell division support our hypotheses.

In our model we assume that all genes are initially associated with H3K4me3 modified nucleosomes, and that accordingly their DNA is unmethylated. Thus, for all genes hyper-methylation can potentially occur. Such behaviour is known from genes associated with CpG islands (Mikkelsen et al. 2007). However, genes associated with short CUs (lengths below a certain threshold) lose H3K4me3 (and H3K9me3) completely independently of initial conditions, and specific systems kinetics and become methylated. These genes mimic genes not associated with CpG islands.

Two groups of genes, here called age-related genes AG1/2, were found to be particular sensitive for changes in systems kinetics. In young cells AG1 genes are associated with H3K4me3 modified, H3K9me3 free chromatin regions of intermediate length (here: $1000 < L < 2000$ bp). AG2 genes are associated with longer H3K4me3 and H3K9me3 modified regions (here: $2000 < L < 3000$ bp). Recently, we demonstrated that these two types of chromatin are frequently found in stem and lineage committed cells (Steiner et al. 2012). In fast cycling (slow histone modifying) cells,

the nucleosomes associated with AG1 genes lose H3K4me3 while those associated with AG2 genes lose H3K9me3. Accordingly, AG1 genes become hyper-methylated and AG2 genes become potentially hypo-methylated in fast cycling (slow histone modifying) cells, providing an explanation of general features of ageing DNA methylation profiles. If the nucleosomes associated with AG2 genes are initially not H3K9me3 modified, these genes conserve their DNA methylation state over the entire ageing process. The same holds for genes associated with even longer CUs. This memory effect is due to bistable H3K9me3 modification states (Binder et al. 2013).

Whether the mechanism underlying hypo-methylation in our model is that observed during *in vivo* ageing remains to be demonstrated. Alternatively, age-related hypo-methylation has been suggested to be a consequence of the hyper-methylation of components of the DNA methylation machinery (Maegawa et al. 2010). Such links between the epigenetic changes, here DNA hyper-methylation, in ageing cells and the emergence of age-related phenotypes are, so far, not considered in our model. Nevertheless, they may strongly impact the ageing process and may open direct or indirect epigenetic pathways towards cancer. On one hand, it is known that during ageing a number of tumour suppressors become silenced, potentially leading to direct tissue transformation (Esteller 2007). On the other hand, silencing of genes, being part of DNA repair mechanisms such as of the MLH1 gene, will increase the mutation frequency of the tissue and thus indirectly facilitate tumour development (Jones & Laird 1999).

In our simulation studies we analysed epigenetic changes following activated proliferation and mutation of parts of the histone modification machinery. The studied scenario of impaired activity of the HDM of H3K9me3 models the DNA methylator phenotype of glioblastoma originating from a mutation of IDH1/2. An analogue DNA methylator phenotype is observed in leukaemia cells. Experimentally, the genes found to be affected are not identical. This is in agreement with tissue specific, age-related methylation profiles (Christensen et al. 2009). Modelling these differences would require considering different activity either of the TF-network or of the epigenetic machineries, or both.

A methylator phenotype has also been detected in colorectal cancer. The origin of the observed hyper-methylation is not known so far. Recent experiments demonstrated that the CpG island methylator phenotype in colorectal cancer is correlated with over-expression of SIRT1, a deacetylase of acetylation of H4 at lysine 16 (Nosho et al. 2009). In proliferative populations such as the intestine (where cells divide on average once a day) the ageing processes described here would take a few weeks only. But, long term age-related drifts in DNA methylation have also been observed in this system (Maegawa et al. 2010). We expect that histone modification rates in fast proliferating systems are much higher, enabling stable inheritance of the modification states.

We have described here the potential interaction between the regulatory systems of histone modification and DNA methylation. Throughout our study we neglected the regulatory impact of histone modifications other than H3K4me3 and H3K9me3. Nevertheless, many aspects of experimentally observed changes of DNA methylation profiles during ageing and tumour development can be explained by our model. However, we expect that further histone modifications critically impact DNA methylation; among them is H3K27me3 (Han & Brunet 2012). The H3K27 HMT recruits DNMTs but binds to unmethylated CpGs and thus appears to fulfil an ambivalent function. Although commonly considered as a repressive mark, silencing so-called bivalent modified chromatin, the mechanism behind is not fully understood. These aspects will be part of future investigations.

Conclusions

The age-related changes in global DNA methylation profiles appear to be, at least in part, a consequence of the limited inheritance of histone methylations. They are established with the cumulative number of cell divisions. However, not only the absolute number of divisions but also the division rate defines the DNA methylation profile. Mutations of the histone modification machinery reorganize the epigenome with respect to these mechanisms.

Funding

This work was supported by the Federal Ministry of Education and Research (BMBF), project grant No. FKZ 031 6065 (HNPCC-Sys) and grant MAGE (grant number 50500541).

References

Akalin A, Garrett-Bakelman FE, Kormaksson M, Busuttil J, Zhang L, Khrebtukova I, Milne TA, Huang Y, Biswas D, Hess JL, et al. 2012. Base-pair resolution DNA methylation sequencing reveals profoundly divergent epigenetic landscapes in acute myeloid leukemia. PLoS Genet. 8(6):e1002781.

Beerman I, Bock C, Garrison BS, Smith ZD, Gu H, Meissner A, Rossi DJ. 2013. Proliferation-dependent alterations of the DNA methylation landscape underlie hematopoietic stem cell aging. Cell Stem Cell. 12(4):413–425.

Binder H, Steiner L, Przybilla J, Rohlf T, Prohaska S, Galle J. 2013. Transcriptional regulation by histone modifications: towards a theory of chromatin re-organization during stem cell differentiation. Phys Biol. 10(2):026006.

Binder H, Wirth H, Galle J. 2010. Gene expression density profiles characterize modes of genomic regulation: theory and experiment. J Biotechnol. 149(3):98–114.

Buratowski S, Kim T. 2010. The role of cotranscriptional histone methylations. Cold Spring Harb Symp Quant Biol. 75:95–102.

Chaturvedi CP, Somasundaram B, Singh K, Carpenedo RL, Stanford WL, Dilworth FJ, Brand M. 2012. Maintenance of gene silencing by the coordinate action of the H3K9 methyltransferase G9a/KMT1C and the H3K4 demethylase Jarid1a/KDM5A. Proc Natl Acad Sci USA. 109(46):18845–50.

Cedar H, Bergman Y. 2009. Linking DNA methylation and histone modification: patterns and paradigms. Nat Rev Genet. 10(5):295–304.

Christensen BC, Houseman EA, Marsit CJ, Zheng S, Wrensch MR, Wiemels JL, Nelson HH, Karagas MR, Padbury JF, Bueno R, et al. 2009. Aging and environmental exposures alter tissue-specific DNA methylation dependent upon CpG island context. PLoS Genet. 5(8):e1000602.

D'Alessio AC, Szyf M. 2006. Epigenetic tete-a-tete: the bilateral relationship between chromatin modifications and DNA methylation. Biochem Cell Biol. 84(4):463–476.

Esteller M. 2007. Cancer epigenomics: DNA methylomes and histone-modification maps. Nat Rev Genet. 8(4):286–298.

Feldman N, Gerson A, Fang J, Li E, Zhang Y, Shinkai Y, Cedar H, Bergman Y. 2006. G9a-mediated irreversible epigenetic inactivation of Oct-3/4 during early embryogenesis. Nat Cell Biol. 8(2):188–194.

Fujita N, Watanabe S, Ichimura T, Tsuruzoe S, Shinkai Y, Tachibana M, Chiba T, Nakao M. 2003. Methyl-CpG binding domain 1 (MBD1) interacts with the Suv39h1-HP1 heterochromatic complex for DNA methylation-based transcriptional repression. J Biol Chem. 278(26):24132–24138.

Grafodatskaya D, Chung BH, Butcher DT, Turinsky AL, Goodman SJ, Choufani S, Chen YA, Lou Y, Zhao C, Rajendram R, et al. 2013. Multilocus loss of DNA methylation in individuals with mutations in the histone H3 lysine 4 demethylase KDM5C. BMC Med Genomics. 6:1.

Han S, Brunet A. 2012. Histone methylation makes its mark on longevity. Trends Cell Biol. 22(1):42–49.

Hayashi-Takanaka Y, Yamagata K, Wakayama T, Stasevich TJ, Kainuma T, Tsurimoto T, Tachibana M, Shinkai Y, Kurumizaka H, Nozaki N, et al. 2011. Tracking epigenetic histone modifications in single cells using Fab-based live endogenous modification labeling. Nucleic Acids Res. 39(15):6475–6488.

Hou J, Wu J, Dombkowski A, Zhang K, Holowatyj A, Boerner JL, Yang ZQ. 2012. Genomic amplification and a role in drug-resistance for the KDM5A histone demethylase in breast cancer. Am J Transl Res. 4(3):247–256.

Jones PA, Laird PW. 1999. Cancer epigenetics comes of age. Nat Genet. 21(2):163–167.

Lu C, Ward PS, Kapoor GS, Rohle D, Turcan S, Abdel-Wahab O, Edwards CR, Khanin R, Figueroa ME, Melnick A, et al. 2012. IDH mutation impairs histone demethylation and results in a block to cell differentiation. Nature. 483(7390): 474–478.

Maegawa S, Hinkal G, Kim HS, Shen L, Zhang L, Zhang J, Zhang N, Liang S, Donehower LA, Issa JP. 2010. Widespread and tissue specific age-related DNA methylation changes in mice. Genome Res. 20(3):332–340.

Mikkelsen TS, Ku M, Jaffe DB, Issac B, Lieberman E, Giannoukos G, Alvarez P, Brockman W, Kim TK, Koche RP, et al. 2007. Genome-wide maps of chromatin state in pluripotent and lineage-committed cells. Nature. 448(7153): 553–560.

Nosho K, Shima K, Irahara N, Kure S, Firestein R, Baba Y, Toyoda S, Chen L, Hazra A, Giovannucci EL, et al. 2009. SIRT1 histone deacetylase expression is associated with microsatellite instability and CpG island methylator phenotype in colorectal cancer. Mod Pathol. 22(7):922–932.

Ooi SKT, Qiu C, Bernstein E, Li K, Jia D, Yang Z, Erdjument-Bromage H, Tempst P, Lin S-P, Allis CD, et al. 2007. DNMT3L connects unmethylated lysine 4 of histone H3 to de novo methylation of DNA. Nature. 448(7154): 714–717.

Przybilla J, Galle J, Rohlf T. 2012. Is adult stem cell aging driven by conflicting modes of chromatin remodeling? BioEssays 34(10):841–848.

Raynal NJ, Si J, Taby RF, Gharibyan V, Ahmed S, Jelinek J, Estecio MR, Issa JP. 2012. DNA methylation does not stably lock gene expression but instead serves as a molecular mark for gene silencing memory. Cancer Res. 72(5):1170–1181.

Reil T. 1999. Dynamics of gene expression in an artificial genome – Implications for biological and artificial ontogeny. Adv Artif Life Proc. 1674:457–466.

Rohlf T, Steiner L, Przybilla J, Prohaska S, Binder H, Galle J. 2012. Modeling the dynamic epigenome: from histone modifications towards self-organizing chromatin. Epigenomics. 4(2):205–219.

Sontag LB, Lorincz MC, Georg Luebeck E. 2006. Dynamics, stability and inheritance of somatic DNA methylation imprints. J Theor Biol. 242(4):890–899.

Sproul D, Nestor C, Culley J, Dickson JH, Dixon JM, Harrison DJ, Meehan RR, Sims AH, Ramsahoye BH. 2011. Transcriptionally repressed genes become aberrantly methylated and distinguish tumors of different lineages in breast cancer. Proc Natl Acad Sci USA. 108(11): 4364–4369.

Steiner L, Hopp L, Wirth H, Galle J, Binder H, Prohaska SJ, Rohlf T. 2012. A global genome segmentation method for exploration of epigenetic patterns. PLoS One. 7(10): e46811.

Takasugi M. 2011. Progressive age-dependent DNA methylation changes start before adulthood in mouse tissues. Mech Ageing Dev. 132(1–2):65–71.

Teschendorff AE, Menon U, Gentry-Maharaj A, Ramus SJ, Weisenberger DJ, Shen H, Campan M, Noushmehr H, Bell CG, Maxwell AP, et al. 2010. Age-dependent DNA methylation of genes that are suppressed in stem cells is a hallmark of cancer. Genome Res. 20(4):440–446.

Thomson JP, Skene PJ, Selfridge J, Clouaire T, Guy J, Webb S, Kerr AR, Deaton A, Andrews R, James KD, et al. 2010. CpG islands influence chromatin structure via the CpG-binding protein Cfp1. Nature. 464(7291):1082–1086.

Turcan S, Rohle D, Goenka A, Walsh LA, Fang F, Yilmaz E, Campos C, Fabius AW, Lu C, Ward PS, et al. 2012. IDH1 mutation is sufficient to establish the glioma hypermethylator phenotype. Nature. 483(7390):479–483.

Vavouri T, Lehner B. 2012. Human genes with CpG island promoters have a distinct transcription-associated chromatin organization. Genome Biol. 13(11):R110.

Velicescu M, Weisenberger DJ, Gonzales FA, Tsai YC, Nguyen CT, Jones PA. 2002. Cell division is required for de novo methylation of CpG islands in bladder cancer cells. Cancer Res. 62(8):2378–2384.

Woo YH, Li WH. 2012. Evolutionary conservation of histone modifications in mammals. Mol Biol Evol. 29(7):1757–1767.

Young MD, Willson TA, Wakefield MJ, Trounson E, Hilton DJ, Blewitt ME, Oshlack A, Majewski IJ. 2011. ChIP-seq analysis reveals distinct H3K27me3 profiles that correlate with transcriptional activity. Nucleic Acids Res. 39(17):7415–7427.

Zhou X, Sun H, Chen H, Zavadil J, Kluz T, Arita A, Costa M. 2010. Hypoxia induces trimethylated H3 lysine 4 by inhibition of JARID1A demethylase. Cancer Res. 70(10):4214–4221.

Appendix

The artificial genome (AG) model

In our simulations we utilize the AG model described in Binder et al. (2010). Deviating parameters are specified in Table A2. We used a realization of the AG with 105 genes. Regulatory interaction between these genes was simulated according to the transcription factor model introduced in Binder et al. (2010). We assume that the AG is wrapped around nucleosomes. As the average gene length in the AG is about 4000 bp and each wrap takes about 200 bp, on average 20 nucleosomes are associated with a gene.

The N_H nucleosomes associated with one gene are assumed to act cooperatively regarding the modification of their histones, i.e. they form a cooperative unit (CU). This is motivated by experimental findings of frequent binding of the DNA-binding molecule CTCF near the transcription start site of genes (Vavouri and Lehner 2012) which has been observed to flank regions of stable histone modification states (Woo & Li 2012). The genes in the AG show an exponential length distribution and thus the CU lengths are exponentially distributed as well.

Accordingly our assumption enables us to study CU length effects in a single simulation. In contrast, effects of the spatial variation of histone modifications around the transcription start site of genes and their impact on their transcription cannot be addressed by our model. Differences in these profiles potentially define subgroups of histone and gene regulatory states (Young et al. 2011) that are not covered by the model.

In order to describe the histone modification process we apply the model described in Binder et al. (2013) and Rohlf et al. (2012) to each of the modifications considered. The chosen parameters are listed in Table A2. In the following, we give a brief description of the model of transcriptional regulation.

Modelling transcriptional regulation

Transcription T_i of the individual gene i of the network is calculated by solving:

$$\frac{\mathrm{d}T_i}{\mathrm{d}t} = P_{\max}\,\Theta_i\,\theta_{\mathrm{Pro},i} - \delta T_i, \tag{1}$$

where δ is a degradation constant and $P_{\max}$ the maximum promoter activity of the gene. Transcription activity of gene i is controlled by the occupancy of its promoter by polymerase II, $\theta_{\mathrm{Pro},i}$, which depends on the properties of the TF network (Binder et al. 2010). In addition, transcriptional activity is assumed to be proportional to the binding probability Θ_i of the protein complex that incorporates the H3K4 HMT to chromatin associated with gene i. This probability is given for the H3K4 and H3K9 HMTs by:

$$\Theta_i = 1/(1 + \exp(\varepsilon_0 + w_{BS,i}\varepsilon_{BS} + n_{HM,i}\varepsilon_{HM})). \tag{2}$$

Here, ε_0 is the ground free enthalpy per bound complex and ε_{BS} and ε_{HM} are the free enthalpy changes of DNA binding and binding to the histone modification, respectively. All these terms are scaled by the Boltzmann unit. For binding of the H3K4 HMT the ground enthalpy is assumed to be proportional to the log-expression of the associated gene:

$$\varepsilon_0 = \varepsilon_1 - \ln\left(\frac{T\delta}{P_{\max}}\right). \tag{3}$$

For binding of the H3K9 HMT it is assumed to be constant ε_2.

The number of modified nucleosomes n_{HM} out of the N_H cooperative nucleosomes associated with the regulatory region of gene

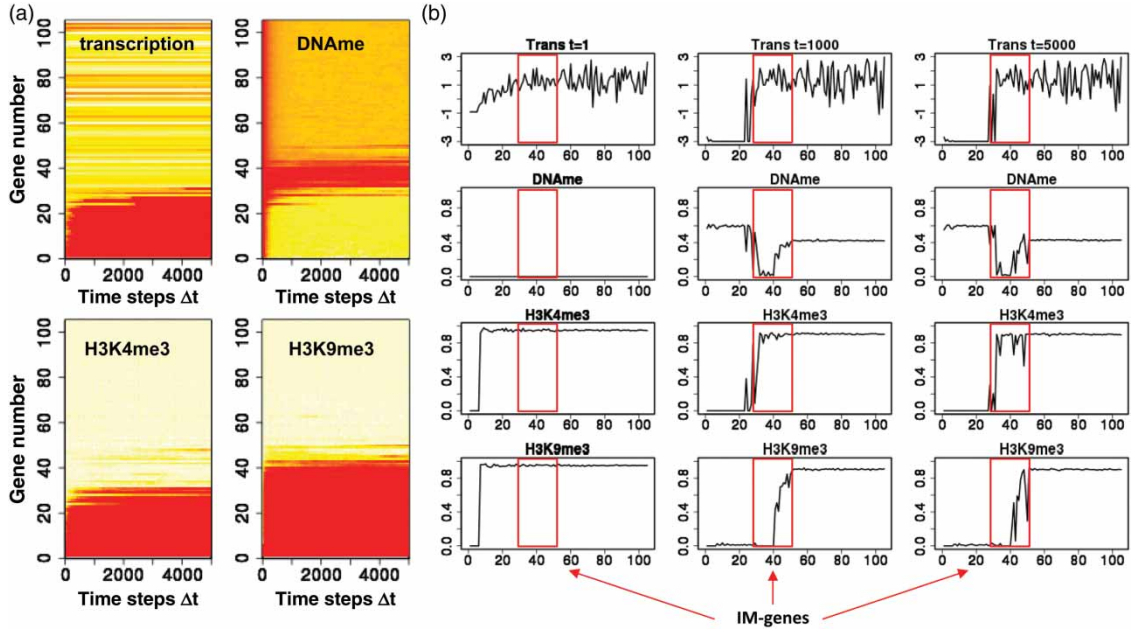

Figure A1. Simulated age-related changes in the epigenome: Modification dynamics. Shown are the results for the same system as in Figure 2 but for fast rates of histone (de-) modification. (a) Regulatory states for each gene are averaged separately over all cells in the population (red–yellow–white: low–high, 100 Δt refers to 1 generation). Normalization and sorting as in Figure 2. The age-related regulatory profile shows the same general features as for slow histone (de-) modification reactions, but the features refer to different genes. IM genes comprise e.g. genes between no. 30 and no. 50. As seen in (b) the impact of the TF network is not that pronounced, as for low rates of histone (de-) modification.

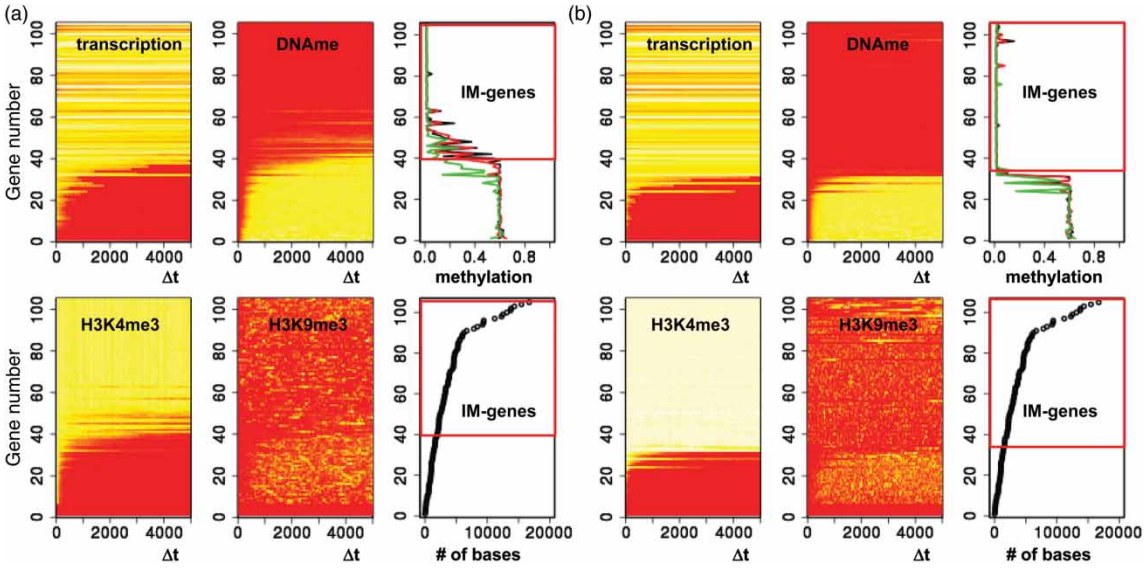

Figure A2. Simulated age-related changes in the epigenome: initial conditions. Shown are the results for (a) low and (b) high rates of histone (de-) modification for the initial state (T1, {1}, {0}, {0}). Regulatory states for each gene are averaged separately over all cells in the population (red–yellow–white: low–high, 100 Δt refers to one generation). Normalization and sorting as in Figure 2. For initially vanishing H3K9me3 this histone modification does not establish over the entire simulation time. As a consequence the DNA of genes longer than the AG1 genes remains unmethylated and the group of IM genes extends to very long genes. The methylation profiles at $t = 1000$ (green line), 3000 (red line), and 5000 Δt (black line) document that the steady state is reached already after 3000 Δt. The gene lengths (length of the CUs) are given in number of bases of the artificial genome referring to the respective gene.

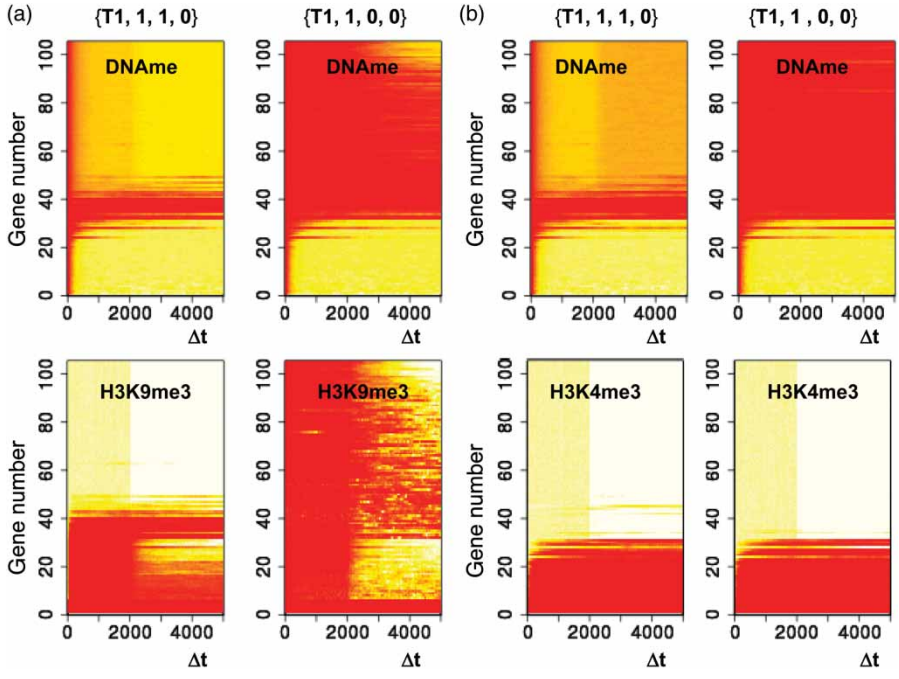

Figure A3. Simulated regulatory states following knock-down of the HDMs. Shown are results for (a) H3K9me3, and (b) H3K4me3 assuming high (de-) modification activity. Subsequent to the knock-down at $t = 2000\Delta t$ an increase of the respective histone modification level is seen. DNA methylation increases for H3K9me3 HDM knock-down and decreases for H3K4me3 HDM knockdown. A large fraction of the genes is affected by the knock-downs.

i is calculated by solving:

$$\frac{\mathrm{d}n_{HM,i}}{\mathrm{d}t} = k_m \Theta_i (N_{H,i} - n_{HM,i}) - k_D n_{HM,i}. \qquad (4)$$

Here, k_D and k_M are the de-modification and modification rate, respectively.

In case of H3K4me3 there is evidence that the HMTs are capable of binding unmethylated CpGs (Thomson et al. 2010).

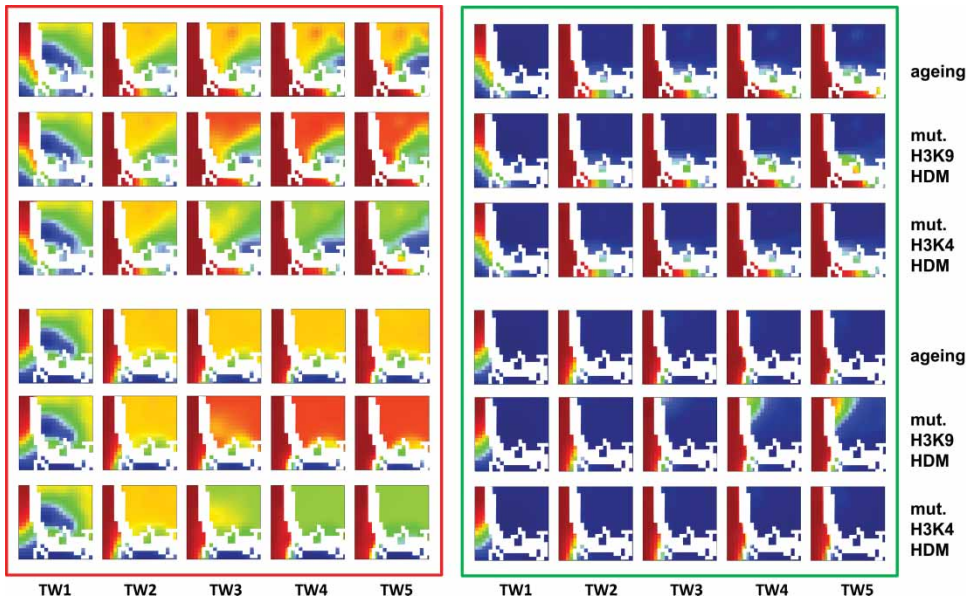

Figure A4. SOM gallery of DNA methylation data. Shown are the SOM portraits of all scenarios (see Table A1) each divided into five time windows (TW). Initial conditions: Red box: (T1, {1}, {1}, {0}), green box: (T1, {1}, {0}, {0}). Histone (de-)modification activity: low (upper three rows), high (lower three rows).

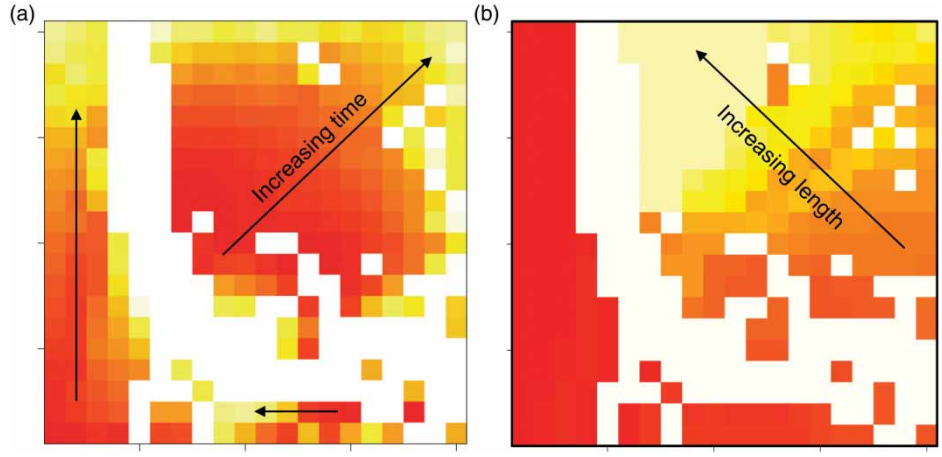

Figure A5. Supporting maps of the SOM analysis. (a) Map of the average time point associated with the meta-elements of the SOM. Each cluster contains meta-elements with SOM profiles that are prototypic for the methylation behaviour of the same gene at different time points. The map colour codes for the average time point of each meta-element. Red: $< 100th$, beige: $> 500th$. (b) Length map of the genes. The average length of the genes in each meta-element is colour-coded. Red: < 1000 bases, beige: > 4000 bases. White meta-elements are unpopulated. Methylation of the genes develops with increasing time in (a). These paths refer to virtually constant lengths in (b). This result show that each gene is characterized by its specific methylation dynamics.

Accordingly; we calculated the average free enthalpy change of DNA binding as $(w_{BS,i}\varepsilon_{BS})$ where $w_{BS,i}$ is the probability of finding a nearby CpG unmethylated. Assuming independent methylation of all CpGs associated with the gene, this probability is simply given by the fraction of unmethylated CpGs. In case of H3K9me3 there is evidence that the HMTs bind methylated CpGs. Thus, the average free enthalpy change of DNA binding was calculated as $(1 - w_{BS,i})\varepsilon_{BS}$. As a result of these assumptions DNA methylation impacts the methylation states of the associated histones.

Modelling DNA methylation dynamics

In order to account for changes of the DNA methylation we applied the basic model of DNA methylation introduced by Sontag et al. (2006) which describes the parallel action of maintenance and *de novo* DNMTs. In this Markov-chain model, CpGs can change their methylation states during cell division only. If a cell is dividing, maintenance methylation ensures that DNA methylation is conserved with a probability D_{main} smaller than 1. Accordingly, not all CpGs keep their methylation status. In addition DNA *de novo* methylation can occur with probability $D_{\text{novo}} > 0$ depending on the modification state of the associated nucleosomes.

Recruitment of *de novo* methylases has been shown to depend on the modification state of the associated histones. In fact, H3K4 methylation has been found to protect associated DNA from becoming *de novo* methylated. On the other hand, H3K9 methylation has been suggested to recruit DNMTs. We introduced a simple interaction model of DNMTs with chromatin depending

Table A1. Simulation scenarios. Overview of the scenarios that have been integrated into the SOM analysis.

	H3K4 and H3K9 $k_M = 0.05$, $k_D = 0.005$			H3K4 and H3K9 $k_M = 0.5$, $k_D = 0.05$		
Initial state	ageing	H3K4 $k_D = 0$	H3K9 $k_D = 0$	ageing	H3K4 $k_D = 0$	H3K9 $k_D = 0$
T1, {1}, {1}, {0}	x	x	x	x	x	x
T1, {1}, {0}, {0}	x	x	x	x	x	x

Table A2. Model parameters. Energy terms are scaled by the Boltzmann unit. Rates are given per simulation time step Δt. The parameters of the AG and the TF network were chosen as in Binder et al. (2010), except of the length of the genome ($L_{\text{genome}} = 4 \times 10^5$) and the length of the base promoter ($L_{\text{prom}} = 6$).

Parameter	Symbols	Values
Ground enthalpy per bound HMT:		
H3K4me3	ε_1	7
H3K9me3	ε_2	10
Free enthalpy change of binding to:		
– unmethylated CpGs: HMT of H3K4me3	ε_{BS}	−5.5
– methylated CpGs: HMT of H3K9me3		−5.5
Free enthalpy change of HMT binding to H3K4me3, H3K9me3	ε_{HM}	−1.5
Modification rate H3K4me3 and H3K9me3	k_M	slow: 0.05 fast: 0.5
De-modification rate H3K4me3 and H3K9me3	k_D	slow: 0.005 fast: 0.05 mutated: 0.0
DNA maintenance methylation probability	D_{main}	0.8
DNA *de novo* methylation probability	D_{novo}	0.3
growth rate (cell divides after 10 growth steps):	R	0.1
mutated:		$6/5\ \text{R} = 0.12$
Differentiation rate	Q	0.0000625
Interaction energy between DNMT and HMT	ε_{K4}	+6
	ε_{K9}	−6
Transcription degradation rate	δ	0.1

on the H3K4 and H3K9 modification status. We assumed the *de novo* methylation rate D_{novo} of a CpG located in the regulatory region of gene i to depend on the modification of the nucleosomes associated with the gene:

$$D_{\text{novo}} = D^0_{\text{novo}}(1 + \exp(-n^{K9}_{HM}\varepsilon_{K9}/N_H))/ \\ (1 + \exp(-n^{K9}_{HM}\varepsilon_{K9}/N_H + n^{K4}_{HM}\varepsilon_{K4}/N_H)). \quad (5)$$

Here, D^0_{novo} is the *de novo* DNA methylation constant for CpGs located in the regulatory region of a gene, where the nucleosomes associated with it are devoid of H3K4me3. ε_{K4} and ε_{K9} are the interaction energies between the DNMTs and the modified nucleosomes scaled by the Boltzmann unit.

Additional simulation results

The following figures provide: (i) results on the systems behaviour for different (de-) modification rates and the initial conditions (Figures A1–2), (ii) detailed data on the system's behaviour following knock-down of HDMs (Figure A3), and (iii) supporting information on the SOM-analysis (Figures A4–5).